INTERNATIONAL JOURNAL OF CONSERVATION SCIENCE
ISSN: 2067-533X Volume 13, Special Issue 1, December 2022: 1535-1552 www.ijcs.ro

NANO-COMPUTED TOMOGRAPHY AS A TOOL FOR THE MORPHOLOGICAL CHARACTERISATION AND VALIDATION OF PAINT MOCK-UPS

Charlotte N. STAHMANN[1,*], Dominik MÜLLER[2], Eva STOREVIK-TVEIT[3], Petra DEMUTH[1], Ester S. B. FERREIRA[1]

[1] Cologne University of Applied Sciences – Cologne Institute of Conservation Sciences, Ubierring 40, 50678 Cologne, Germany
[2] University Würzburg/IIS Fraunhofer, Josef-Martin-Weg 63, 97074 Würzburg, Germany
[3] MUNCH, Edvard Munchs Plass 1, 0194 Oslo, Norway

Abstract

The development of new conservation treatments is ideally carried out on model systems, so-called mock-ups, thus avoiding direct testing on cultural heritage objects. Additionally, mock-ups allow for statistically significant test results as they provide unlimited, reproducible test material. They are prepared with similar or same classes of materials as identified in the objects they try to mimic. In the case of paint mock-ups, used for the development and assessment of consolidation methods, the creation of model systems with similar morphology, including porosity, is optimal, even if technically challenging. To produce paint mock-ups, representative for a painted area of the painting "Beach Landscape with Trees and Boats" (1905-06) by Edvard Munch, microsamples of the target area were analysed with a combination of analytical methods. FTIR and Py-GC-MS were used for the identification of pigment and binder and nano computed X-ray tomography (nano-CT) for the characterisation of the porosity. The pigment and binder were identified as synthetic ultramarine blue and casein, respectively. The pigment-binder ratio was estimated based on the FTIR spectra. According to the results, three mock-up types were prepared with three different types of synthetic ultramarine blue pigments: two commercially available and one historical synthetic ultramarine blue pigment from the MUNCH's collection of historical art materials by E. Munch. To compare their porosity, tomography on samples of the original and the three mock-up types was performed using a laboratory-based nano-CT setup. The results showed that all tested synthetic ultramarine blue pigments have distinct particle size distributions. Thus, none of the model systems exactly could reproduce the porosity found in the original. However, the combination of results on chemical composition, approximate pigment-binder ratio, porosity, and pigment particle size distribution allowed the selection of the model system which properties were closest to those of the original.

Keywords*: Paint mock-ups; Morphology; Porosity; Nano computer tomography; Synthetic ultramarine blue pigment*

Introduction

Physical model systems, also known as mock-ups or reconstructions, play a fundamental role in art technological, conservation and conservation science studies. They can be helpful in the investigation and study of artists' techniques, material reactivity, ageing mechanisms and in the development and evaluation of new conservation and restoration materials and methods, without directly affecting the original cultural heritage object [1-10]. The creation of suitable

* Author for correspondence: charlotte.stahmann@gmail.com

mock-ups that reproduce the chemistry and physical properties of the original is challenging but crucial for the relevance of the obtained results.

When mock-ups are prepared for the simulation of conservation treatments, in which the absorbency of the materials plays a role, not only the chemical composition and layer build-up should be considered but morphological properties such as porosity are equally important. This is for example the case for consolidation treatments in which porosity has a decisive impact on the imbibition of the liquid consolidant [11, 12].

In the current study, paint mock-ups were produced aiming to mimic a cohesively weak dark blue paint area from the painting “Beach Landscape with Trees and Boats” (Woll 637), painted 1905-06 by Edvard Munch, in terms of materiality and porosity.

The developed model system was used to evaluate low molecular weight cellulose ethers comparatively and systematically as consolidants for this specific paint layer. The results of that study are presented elsewhere in the current special issue [13].

Case Study "Beach Landscape with Trees and Boats"

Edvard Munch painted “Beach Landscape with Trees and Boats” (Woll 637, MUNCH, Oslo) (Fig. 1) in 1905-6. The motive shows a clear resemblance to his two other paintings on canvas “Beach Landscape with Trees and Boats” (1905-06, Woll 636, MUNCH, Oslo) and “Trees by the Sea” (1906-07, Woll 727, Neue Nationalgalerie, Berlin). The latter is part of the so-called Reinhardt Frieze, which was commissioned in 1906 by Max Reinhardt for the entrance hall of the Deutsches Theater Berlin [14].

The here presented version of “Beach Landscape with Trees and Boats” (Woll 637) is painted directly on an unprimed canvas. The paint layer does not completely cover the support, leaving the bare fabric exposed in several areas.

Fig. 1. Edvard Munch, “Beach Landscape with Trees and Boats” (Woll M 637, MUNCH, Oslo), 1905-06, 89.5x138.5 cm, with markes to locate the areas of the detail images (left, photo: O. Kvavik), three microscopic detail images of the yellow, light blue and dark blue paint layers (right)

The condition of the different painted areas varies. The yellow and light blue areas show cracking, extensive crumbling, and pigment loss upon abrasion, indicating the paint layer’s weak cohesion and adhesion to the support. These areas have already suffered severe losses. In contrast, the dark blue paint layer consists of a coherent layer. It has been applied evenly by brush in a single layer onto the canvas support, resulting in a ~200µm thick dry paint film.

The adhesion of the paint layer to the substrate is sufficient. However, the cohesion is rather low and pigment grains detach from the surface when gently abraded with a white silicon tip (Colour Shaper®).

Underbound paint layers and consolidation

The fragility of the paint layers in "Beach Landscape with Trees and Boats" can be associated both with the painting technique and ageing processes within the materials used. Munch applied paint with a low amount of a water-based binding medium directly on absorbent not primed canvas, to achieve the desired matt appearance of the paint surface [15, 16]. In water-based physically drying binding media, such as animal glue or casein, the binding medium dries gradually through solvent evaporation. Proteinaceous binding medium solutions commonly contain a low solid content (<7%).[1] This means that upon drying, only a small amount of polymer is available to bind the pigment particles. Building upon the model proposed by Michalski [12], figure 2, attempts to schematise this process. Consequently, physically drying, water-based binding media such as proteins have often been identified in fragile and cohesively weak paints [17]. The absence of a continuous binder film in which the pigment particles are fully embedded means that the light is scattered at the layer surface rather than being reflected [18], creating a matt appearance strived for by artists in the late 19th and early 20th century [15, 16, 19, 20].

The exposure of the binder to environmental factors, when present only in isolated bridges between pigment particles, is high. Several parameters may lead to the deterioration of the binding medium in the paint layer, making a consolidation treatment necessary [13].

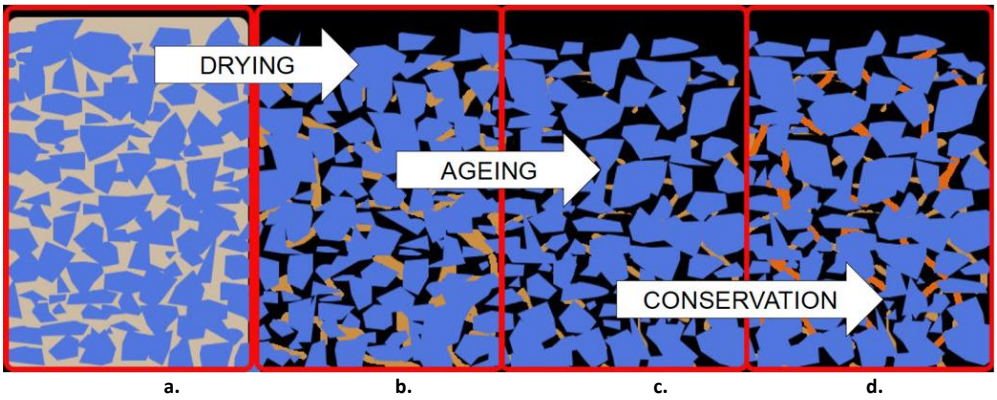

Fig. 2. a. Pigments dispersed in aqueous proteinaceous binder (polymer and solvent) applied as wet paint on a support; b. The drying of the paint involves evaporation of the solvent. When the solvent has completely evaporated only the binder remains, building binder-bridges between the pigment particles; c. With ageing and exposure to mechanical and chemical stresses the binder bridges may swell and shrink and the paint system may lose its cohesion; **d.** After the consolidation treatment, the evenly distributed consolidant forms new polymer bridges or reinforces degraded ones, resulting in an increased paint layer cohesion ideally without changing the appearance of the paint layer

In consolidation treatments, liquid consolidants (consisting of polymer and solvent) are applied onto the paint layer's surface and imbibe the paint layer driven by capillary pressure. Ideally, the liquid consolidant will imbibe the paint layer, and, after evaporation of the solvent, form evenly distributed new bridges between particles or reinforce existing ones (Fig. 2d.). Although the distribution of the consolidant in paint layers has been observed experimentally [13, 21], the exact localisation of the added consolidant polymer, either as particle coating or new nanobridges, remains unknown. Figures 2b-c. are illustrative models.

[1] Doerner e.g., recommends a solid content of 5% for casein (p. 178), ca. 4-6 % for gelatine (p. 180) and ca. 6,5% for other animal glues (p.98). [42]

The imbibition of liquids in a porous medium is a complex process. It is influenced by the properties of the liquid such as viscosity, surface tension (liquid-gas interfacial tension) and density; by the properties of the porous substrate such as its surface free energy (solid-gas interfacial tension), pore connectivity (effective porosity), tortuosity, pore radii, and pore geometry; and by the contact angle, which is measured at the three-phase contact line where the tangential forces caused by the interfacial tensions (liquid-gas, solid-gas, liquid-solid) are in equilibrium. Gravity and boundary effects, as well as evaporation and possibly swelling, occurring simultaneously to imbibition, also play a decisive role [22].

X-ray tomography in the characterisation of porosity in microsamples

As discussed previously, porosity plays a fundamental role in the imbibition process. Porosity is defined as the void volume divided by the total volume of a porous medium in percentage (total porosity [%] = (void volume/total volume) x 100). The total porosity of paint layers is determined by the pigment's particle shape, the average particle size, the particle size distribution, and the amount of present binding medium. However, not all voids (pores) in a porous medium are interconnected. This is particularly important in the context of consolidation, as fluids can only flow through a permeable porous media with interconnected voids. The resulting effective porosity (effective porosity [%] = (interconnected void volume/total volume) x 100) is often smaller than the total porosity [23].

For the above discussed reasons, the characterisation of the porosity of the original paint layer and of the mock-ups is important to evaluate their suitability as models for investigations of consolidation treatments. Since only microsamples can be collected from the painting, methods such as mercury intrusion porosimetry (MIP) [24] are not suitable. X-ray microtomography has been used to characterise porous media in multiple materials of cultural heritage [25, 26], including paint and ground layers on paintings [27-30].

In previous studies, the potential of X-ray tomography for porosity characterisation in microsamples from paintings has been discussed [27, 30]. In the earlier paper Ferreira et al. reported on the use of synchrotron X-ray tomographic microscopy (SRXTM) to visualize the porosity of painting grounds at a pixel size of 370nm [30]. The later paper dealt with the quantitative characterisation of porosity aspects and connectivity [27].

In addition to established synchrotron methods, X-ray tomography techniques with significant sub-µm resolution have become established in the laboratory environment in recent years. From an instrumental perspective, different methods are available for laboratory-based nano-CT. These include lens-based full-field microscopes [31] as well as devices that use projection-based magnification, either with adapted SEM devices as the source [32] or with a nano focus X-ray source [33]. With these devices, 3D resolutions in the range of 50-150nm can be achieved.

Materials and methods

To systematically investigate the impact of parameters such as viscosity, surface tension, application method and applied quantity of the consolidant solution on the imbibition depth and the resulting cohesion of the target paint layer from Munch's painting "Beach Landscape with Trees and Boats" (Woll 637), the preparation of mock-ups was required [13]. As a first step, the painted area to be reconstructed was characterised in terms of canvas type, binder and pigment chemistry and their relative ratio, pigment particle size distribution and porosity. For the first time in that context, laboratory-based nano computed X-ray tomography was used.

Characterisation of canvas and paint samples from E. Munch's painting

Weave structure and fibre analysis

To characterize the canvas structure of the original painting and for finding a similar fabric for the preparation of mock-ups, a weave structure analysis according to Rouba [34] and a modified Herzog test using a polarized light microscopy (PLM Leica DM750P) were performed.

The Herzog test provides information on the bast fibres' fibrillar orientation (S- or Z-twist) responsible for the specific interference-colour in dependence on the fibres' position in the PLM. Flax and nettle fibres, both with a S-twist microfibrillar orientation, show a blue interference colour when in horizontal position and a red interference colour when in vertical position. The contrary is the case for the Z-twisted microfibrils in hemp fibres. For a detailed description of the test method see *E. Haugan and B. Holst 2013, p. 166* [35] and *Wülfert 1999, p. 290 and 352* [36]. For the Herzog test, each three fibres from the original canvas' horizontal and vertical thread systems were taken.

FTIR (pigment and binder analysis, measurement of pigment-binding medium ratio)

For the pigment and binding medium analysis and for the measurement of the approximate pigment-binder ratio, a Thermo Nicolet 4700FT-IR Spectrometer coupled to a Continuum microscope was used. The samples were compressed in a diamond anvil cell and analysed in transmission mode. With a spectral range of 4000-600cm^{-1} and a spectral resolution of 4cm^{-1} a total of 128 scans was collected. The data was processed using Software OMNIC 8 *(Thermo Fisher Scientific)*.

To determine the approximate pigment-binder ratio of samples from the dark blue paint layer in Munch's painting, a calibration plot was generated using the ratios of characteristic absorption band intensities of mock-ups prepared with a protein binder and synthetic ultramarine blue in known quantitative composition. The peak intensities (peak heights) of the absorption bands at wavelength 1651cm^{-1}, characteristic for proteins (amide I band), and at 657cm^{-1}, characteristic for ultramarine, were measured after baseline correction in OMNIC 8. For each spectrum the ratio of the maximum peak intensities was determined and used to generate a calibration plot (peak intensity ratios versus binder concentration).

This method is based on that the intensity of each absorption band is directly proportional to the concentration of the absorbing group [37]. The measurement of peak intensities has been used in previous studies for monitoring and comparing chemical changes in mock-up paint layers during artificial ageing [38]. In another study, the area of the absorption bands has been used instead of the peak intensities for determining the binder concentration in paint samples [39].

The nature of the protein had not been determined at the stage of these measurements. Therefore, the calibration was carried out using samples with synthetic ultramarine blue dark (#45010, *Kremer Pigmente*) and hide glue (*Kremer Pigmente*) at different concentrations (2%, 3% and 6%) 2:1 (w/w), applied on Hostaphan® polyester foil RN 75, 105g/m². For each concentration 2-3 samples were collected and analysed in duplicate.

Py-GC-MS

Py-GC-MS analysis of the original Munch sample was carried out by Jennifer Poulin at the Canadian Conservation Institute in Ottawa. Pyrolysis was performed using Direct Inlet pyrolysis-gas chromatography-mass spectrometry (DIP-GC-MS) following the procedure described in *J. Poulin et al. 2022* [40]. As a sample reagent 2µL tetramethylammonium hydroxide (TMAH, *Supelco, Bellafonte, PA, USA*) (2.5% in methanol) was used.

SEM

The Scanning Electron Microscope (SEM) Sigma VP (*Zeiss*) was used to image the surface of the original Munch sample and the mock-up prepared with synthetic ultramarine blue dark (#45010, *Kremer Pigmente*) and 3% casein (w/w) 2:1. The samples were coated with platinum using the coating system Q150T ES (*Quorom*). Measurements were carried out using an InLens SE detector and an acceleration voltage of 2kV.

Preparation of the mock-ups

In the following, the methodology used for producing the paint mock-ups trying to reproduce a chosen paint area in Munch's painting "Beach Landscape with Trees and Boats" (Woll 637) will be described in detail.

Pigments. For the test mock-ups three different kinds of synthetic ultramarine blue pigments ($Na_8Al_6Si_6O_{24}S_3$ [41]) were used. Two modern and commercially available synthetic

ultramarine blue pigments by *Kremer Pigmente*, very dark (#45000) and dark (#45010) (Table 1) and for comparison a historical synthetic ultramarine blue pigment from MUNCH's historical material collection by E. Munch (Fig. 1), were used. For the final production of mock-ups, synthetic ultramarine dark (#45010) was chosen.

Table 1. Information from the data sheets of the two commercially available synthetic ultramarine blue pigments from Kremer Pigmente

Pigments	Density	Tamped Density [g/cm^3]	Oil number* [mL per 100 g Pigment]	Average particle size [µm]
synt. ultramarine blue dark (#45010)	2.3	0.8	45	2.5
synt. ultramarine blue very dark (#45000)	2.35	0.84	32	3.8

*The oil number is defined as the amount of oil (ml) needed to bind 100 g of pigment to a paint paste that can be spread on a glass plate without breaking and without detaching from it (DIN EN ISO 787-5:1995-10).

Binding Medium. As a binding medium casein powder (#7555.2, *Carl Roth*) was used and prepared as described by Doerner [42] using ammonia solution and deionised water (for a detailed description see below).

Canvas. For the selection of the canvas several commercially available linen canvas types were compared with the original. Finally, *D.M. 18 puro lino* from *Tessitura Enrico Sironi* was chosen. The textiles warp threads are delivered with a sizing of polyvinyl alcohol, and the weft yarn occasionally with paraffin wax to improve the performance of the weaving loom.[2]

Further Materials for the Mock-up preparation. As a support for the canvas pieces honeycomb-carton (supplied by *Klug* in 9x15cm pre-cut pieces) was used and applied with BEVA® 371 film (thick, 65µm).

Step-by-step description of mock-up preparation

The test mock-ups which were analysed with nano-CT in this study were prepared in the same way as the 65 mock-ups which were used for the systematic investigation of consolidation methods and materials [13]. **STEP 1** The canvas, neither washed nor decrimped, was cut into pieces of 9x15cm, with the warp threads parallel to the long side of the textile pieces. **STEP 2** BEVA® 371 film was applied to the honeycomb cardboard (9x15cm) by heat activation (iron at 75°C) and then cooled down under pressure using a glass plate and weights. In a further step, the canvas pieces were applied to the BEVA® 371 coated honeycomb cardboard by heat activation and again cooled down under pressure. **STEP 3** The casein binder was prepared according to Doerner [42]: 15g casein powder was left to swell in 75g deionised water for 24 hours (at 7°C). The solution was heated to 45°C and 3g ammonia solution (25%) was added, leading to a change of the solutions consistency to a thick substance with a yellowish color. On the following day, the casein solution was diluted down to a solid content of 3% with deionised water. **STEP 4** For the preparation of the paint, 20g of the pigment was mixed with 4.5g of deionised water using a glass muller on a glass plate. After complete wetting of the pigments, 10g of the 3% casein solution were added and mixed until no lumps remained. **STEP 5** An automatic film applicator (*byko-drive G, 10mm/s, BYK Additives & Instruments*) and a four-fold film applicator frame (*BYK Additives & Instruments*) with a gap height of 150µm were used for the paint application. Before each new application, the film applicator frame was filled with 15ml of liquid paint and then pushed over the canvas with automatic film applicator (10mm/s). The top and bottom edges of the test canvas were masked with masking tape (*Economy, tesa*) to prevent the paint from penetrating the fabric and cardboard.

Due to the weave structure of the canvas the thickness of the dried paint layers varied from 150-450µm.

Characterisation of the paint layer's morphology

[2] The information was provided by Tessitura Enrico Sironi via e-mail on the 27.6.22.

Nano-CT

Samples of the resulting three test mock-up types and the original (Table 2) were investigated for their porosity using the laboratory-based computed nano tomography instrument ntCT developed at Fraunhofer EZRT [33]. Its high resolution is based on a nanofocus X-ray source and geometrical magnification. The X-ray source is a Excillum Nanotube with a 500nm thick tungsten transmission target. A DECTRIS EIGER2 R direct photon counting detector based on a CdTe sensor with an active area of 2070x514 square pixels, each 75µm wide, was used for image acquisition. The detector is placed on a 3 degrees of freedom manipulator at distances between 180-650mm from the X-ray source to achieve a magnification from several micrometers down to 50nm voxel sampling. For detailed information about the instrument see *D. Müller et al. 2021* [33].

The samples had a size of max. 400µm and were mounted, with the surface facing up, onto the tip of a needle-shaped sample holder using epoxid resin (*UHU Plus Endfest 300*). The two-component resin was pre-cured for 120 minutes and applied in a small quantity onto the sample holder, before collecting the sample and letting it dry in inverted position.

The measurements of the four samples (Table 2) have been scheduled over a longer period of the project duration. In parallel, the prototype of the CT system used was continuously developed and improved.

Table 2. Overview of samples measured with nano-CT.\

Sample No.	Sample Description
M1	Original sample from "Beach Landscape with Trees and Boats" (1905-06), E. Munch
R1	Mock-up synt. ultramarine blue (MUNCH's historical material collection) in 3% casein, 2:1 (w/w)
R2	Mock-up synt. ultramarine blue dark (Kremer Pigmente) in 3% casein, 2:1 (w/w)
R3	Mock-up synt. ultramarine blue very dark (Kremer Pigmente) in 3% casein, 2:1 (w/w)

The acquisition parameters applied are summarized in Table 3. For each sample, the best imaging parameters selected to the best of our knowledge at that time were applied. The considerable variations in the acquisition parameters are therefore not caused by the specific sample but rather by the state of development of the analysis device. Reconstruction of the radiographic images was performed using a proprietary instrument-specific software based on filtered back projection algorithms. During this step, the measurement data was corrected for various disturbing effects that inevitably occur during nano-CT, such as sample drift, detector inlinearities, or beam hardening. A subsequent phase retrieval and an additional post-ring filter were applied to the data in pyXIT [43]. The evaluation, further processing and display of the 3D data was carried out in *Thermofisher Avizo* software based on grey scale segmentation.

Table 3. Overview of acquisition parameters for the computed tomography measurements with information on source distance (SOD), source-detector distance (SDD), number of exposures, effective sampling size, single image exposure time, detector energy window (upper and lower threshold), power on the X-ray target and acceleration voltage

Sample No.	General Settings				Detector		Source	
	SOD (mm)	**SDD (mm)**	**Recordings (Count)**	**Sampling (nm)**	**Exposure Time (s)**	**Threshold Window (keV)**	**Target Power (mW)**	**Voltage (kV)**
M1	0.60	275	1500	160	15	5 - 60	79	60
R1	0.48	350	2400	103	12	5 - 110	954	110
R2	0.60	450	2400	95	22	5 - 60	68	60
R3	0.60	275	1500	160	15	5 – 60	73	60

Results and discussion

Weave Structure and Fibre Analysis

The canvas support of the painting "Beach Landscape with Trees and Boats" (Woll 637) was examined in a framed condition. It was not possible to check the cutting edges of the fabric for a selvedge, thus, warp and weft threads could not be identified. In the following they will therefore be named vertically and horizontally running threads.

The canvas has a plain weave with 12x12 threads per cm^2, an average thread diameter of 0.51cm (vertical threads) and 0.56cm (horizontal threads), a vertical fabric fills of 61.2%, a horizontal one of 67.2% and a total fill of 87.27 % (Table 4).

Table 4. Overview results weave structure and fibre analysis of the canvas in "Beach Landscape with Trees and Boats" (E. Munch, 1905-06) and the canvas used for the paint mock-ups

Canvas	**Beach Landscape with Trees and Boats**		**„D.M. 18" puro lino**	
Fibre type	Flax (or nettle)		Flax	
Weave	Plain weave		Plain weave	
Thread orientation	**Vertical**	**Horizontal**	**Vertical**	**Horizontal**
Thread counts per cm^2	12 threads/cm	12 threads/cm	11 threads/cm	11 threads/cm
Thread twist and angle	Z, 61.2°	Z, 63.9°	Z, 61°	Z, 56,3°
Average thread diameter	0.51±0.09mm	0.56±1.70mm	0.54mm	0.55mm
Fabric Fill cf. [34]	61.2%	67.2%	59.4%	60.5%
Total Fabric Fill cf. [34]	**87.3 %**		**84.0%**	

The six fibres analysed with the Herzog Test using a PLM all showed a blue interference colour when in horizontal position and a red interference colour when in vertical position (Fig. 3), indicating the presence of flax or nettle fibres. As the use of nettle textiles as painting supports is not common, it was presumed that the original support is a flax (linen) textile. However, for a precise identification a complementary microscopic investigation of the fibres' cross section is necessary [44].

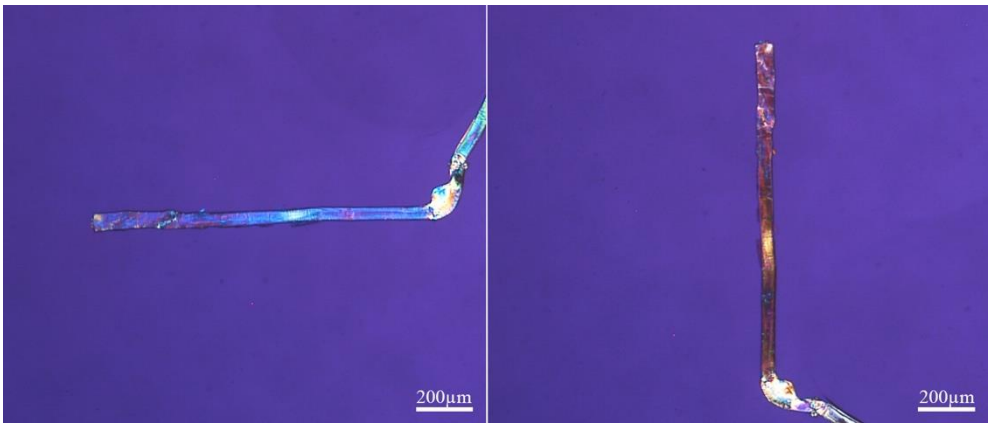

Fig. 3. Images of fibre taken from the canvas of Munch's "Beach Landscape with Trees and Boats" under the PLM (Leica DM750P) showing the characteristic blue and red interference-colour when in horizontal or vertical position, respectively

To find a textile for the mock-up preparation that comes close to the original, weave structure analysis of six modern linen canvas textiles were carried out. The linen fabric *D.M. 18 puro lino* from *Tessitura Enrico Sironi*, matched closest (Table 4).

Binding Medium and Pigment Analysis (FTIR, Py-GC-MS)8

FTIR showed that the pigment is a synthetic ultramarine blue pigment, with an absorption band at 657/693cm^{-1} in the fingerprint region, and that the binder is proteinaceous, with an absorption band at 1651cm^{-1}, proving the presence of amino groups (Fig. 4).

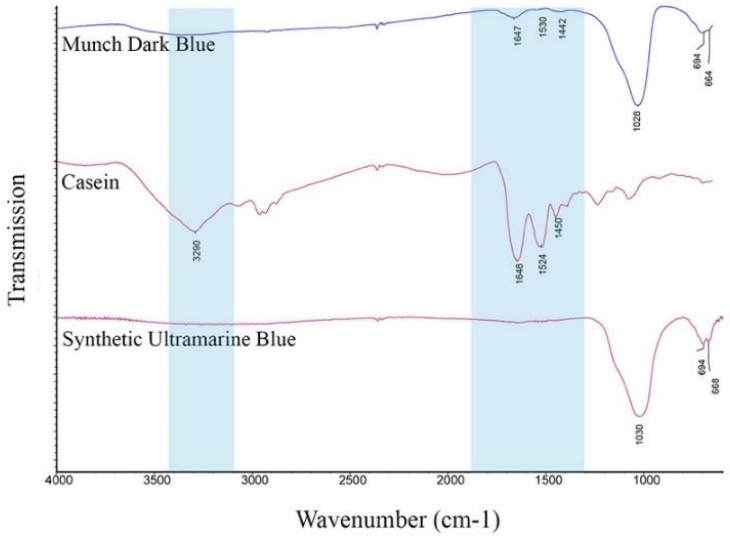

Fig. 4. FTIR spectra of a sample taken from the dark blue area of "Beach Landscape with Trees and Boats" (E. Munch 1905-06) and reference of protein and synt. ultramarine

In the FTIR spectra the bands assigned to the amide bonds, which are the link between each amino acid within a protein chain, were identified. They include NH stretching vibrations, associated with the amide A band, C=O stretching vibrations, as well as C-N-H bending, and CH bending, associated with the amide I, II and III bands.

Although the sample was small and the resultant Py-GC-MS chromatogram was weak, several protein pyrolysates were detected. These include 2,5-diketopyrrole (m/z 93, 186) and a diketopiperazine (DKP) compound that has been identified both as originating from proline-alanine by *S. Orsini et al. 2017* [45] and from alanine-valine by *J.-H. Wang et al. 2010* [46] (m/z 70, 97, 125, 168). A third prominent protein marker present in the chromatogram has yet to be identified (m/z 70, 139, 168). This marker is the most diagnostic for the paint sample because it is the key pyrolysate in casein protein reference materials that have been derivatised using TMAH [47]. The presence of a high relative abundance of this unidentified marker, as well as the absence of certain other protein markers, such as DKPs from proline-glycine and proline-proline, indicates that the paint binder is casein.

Reassuringly the materials identified in the sample are present among MUNCH's collection of painting materials found in E. Munch's studios after his death, including paint tubes, crayons, palettes, varnish and binder bottles, inks, loose pigments, watercolours and more [48, 49]. Amidst those were three bottles of casein solution (*Kaseinopløsning nr. 1036 F*) by *Alf Bjerckes Fernissfabrikk* and a paper bag filled with synthetic ultramarine blue pigment (Fig. 5). The presence of loose pigments and binding medium products in MUNCH's historical material collection as well as bills from their purchase and written records from Munch's contemporaries give evidence for Munch's use of self-prepared paints [16, 50]

Fig. 5. Painting materials by E. Munch from MUNCH's collection. Three bottles of casein binder from *Alf Bjerckes Fernissfabrikk* and a box filled with loose pigments in paper bags, among those a bag of synt. ultramarine blue pigment

Pigment-Binding Medium Ratio

The scattering of the measurements of samples collected from different areas in the test mock-ups (prepared with 2%, 3% and 6% hide glue in a 1:2 ratio (w/w) with synthetic ultramarine blue pigment) and in the original was significant (Fig. 6).

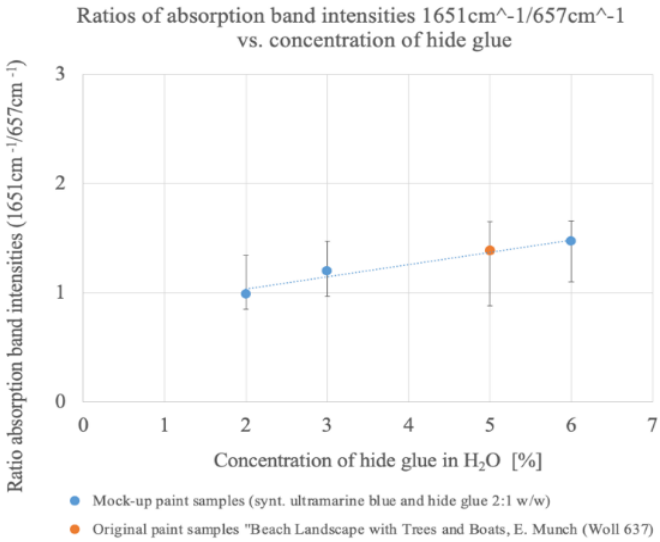

Fig. 6. Calibration plot with ratios of FTIR absorption band peak intensities of paint samples from mock-ups prepared with synt. ultramarine blue and hide glue in different concentrations 1:2 (w/w) (blue) and band intensity ratio of paint sample from "Beach Landscape with Trees and Boats" (orange)

This indicates that the protein binder in the mock-up paint films, and the original is not evenly distributed within the paint layer. This signifies that the obtained value remains an approximation and that the exact concentration cannot be determined accurately without further

analysis of a statistically significant number of samples. Using the calibration plot it can be determined that the average pigment-binder ratio of the original paint layer comes close to a mock-up paint film prepared with a 5% hide glue solution in 1:2 (w/w) mixture with synthetic ultramarine (Fig. 6).

Since the synthetic ultramarine blue used in the mock-ups and used for the creation of the calibration plot, contained a small amount of kaolin, the real ratio of organic to inorganic material of the original paint sample is lower. Paint films prepared with a binder concentration of >3% already showed a too high cohesion for being suitable mock-ups for studies on the effectiveness of consolidants. For those reasons and to create paint layers with a lower cohesion, the mock-ups were prepared with 3% casein solution in 1:2 (w/w) mixture with synthetic ultramarine blue.

Perspectively, accelerated ageing of mock-ups with higher binder concentrations should be considered to create mock-ups that are a more accurate representation of the original.

Visualization of Binding Medium in underbound paint layers

Scanning electron microscopy (SEM) images of the surface of an original paint sample and the mock-up paint prepared with synthetic ultramarine blue dark (#45010, *Kremer Pigmente*) show that no continuous binder film is present and that the paint cohesion results from the presence of isolated organic binder bridges in the nanometre range (Fig. 7).

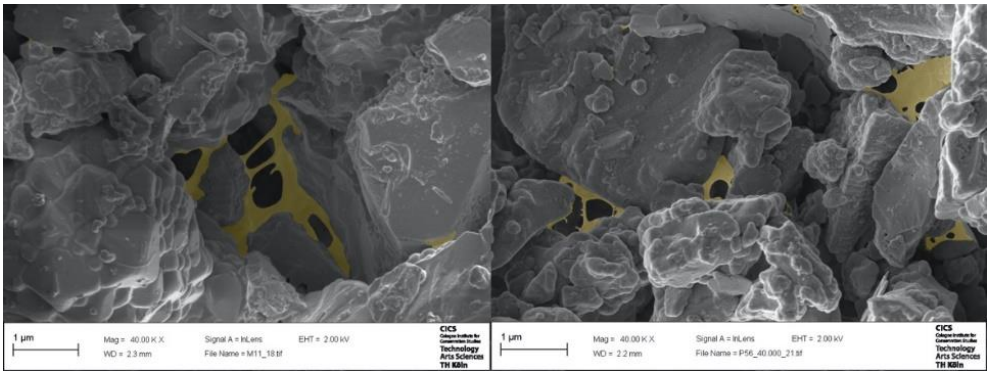

Fig. 7. SEM image with 40,000 x magnification of paint sample surface of ”Beach Landscape with Trees and Boats” (left) and paint mock-up surface prepared with synt. ultramarine blue dark (#45010, *Kremer Pigmente*) and 3% casein (w/w) 2:1 (right), the binding medium bridges are highlighted in orange

It is expected that this is also the case for the bulk paint, however, the distribution of binding medium within a porous paint layer has so far not been experimentally described.

Morphology (Pigment Particle Shape and Distribution and Porosity)

In the obtained nano tomograms (Fig. 8) two phases, the void and the pigment, can be distinguished by their different grey values caused by the deviating photon absorption of the materials. Additionally, the original paint sample by Munch includes a small fraction of higher density particles with strong absorption.

According to the SEM images, the only weakly absorbing binder forms predominantly thin bridges between the particles, most of which are below the resolution limit of the instrument. Therefore, the binder can only be partially segmented which is not sufficient for an accurate investigation. The binding medium and air phase were therefore combined in contrast to the pigment phase (Fig. 8).

From the segmented data, information on the particle shape (length/width), average particle size, particle size distribution and on total porosity (binder and voids) was derived. For the evaluation of the average particle size and particle size distribution the equivalent diameter was used. The equivalent diameter is here equal to the diameter of a sphere having the same volume as an irregularly shaped pigment particle.

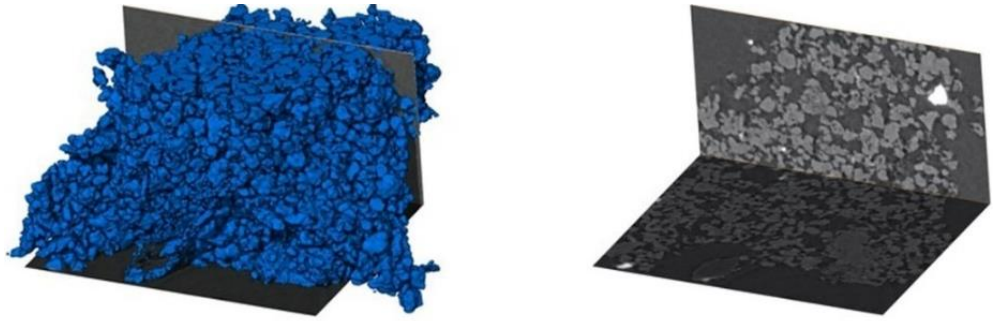

Fig. 8. Reconstructed nano-CT scan with rendered volume of the original Munch sample M1 (left) and unrendered orthogonal sectional images of same sample (right)

The particles of all investigated paints show predominantly an elongated shape with an aspect ratio of approx. 1:1.7 (Fig. 9, Table 5).

All pigments have a low peak in the region of very small pigment particles followed by a wider distribution in the region of larger pigment particles (Fig. 9).

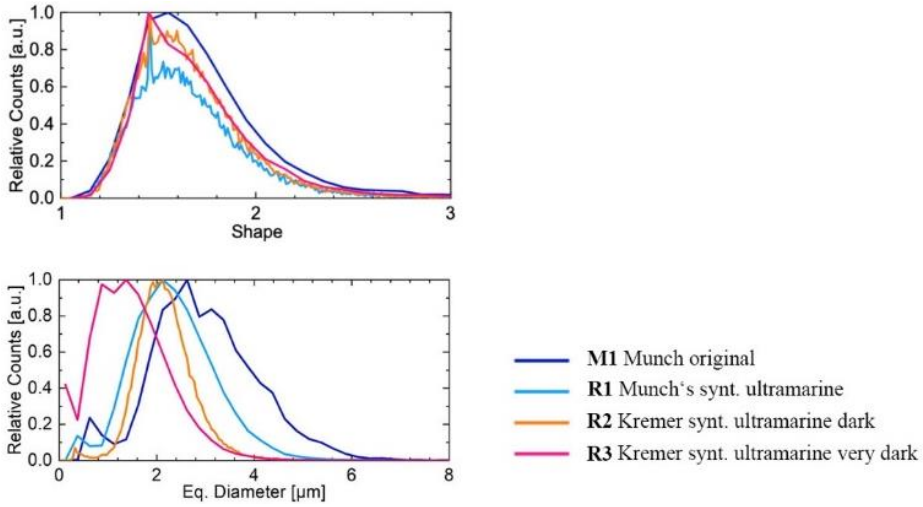

Fig. 9. Particle shape length/particle size width (with 1 corresponding to a sphere) and the equivalent particle diameter extracted from nano CT scans of paint samples from M1, R1, R2 and R3

Table 5. Statistics of nano CT data analysis with mean, min. and max. values of the eq. diameter and particle shape of samples M1, R1, R2 and R3

Pigment Type	Beach Landscape with Trees and Boats	Synt. ultramarine pigment MUNCH collection	Synt. ultramarine blue pigment dark	Synt. ultramarine blue pigment very dark
Binding Medium Type	Casein binder 3% in water 1:2 w/w pigment			
Sample No.	**M1**	**R1**	**R2**	**R3**
Mean eq. Diameter (µm)	**2.98**	**2.35**	**2.18**	**1.47**
Min. Eq. diameter (µm)	0.36	0.13	0.11	0.2
Max. Eq. diameter (µm)	10.52	10.89	9.48	8.3
Mean Shape	**1.72**	**1.67**	**1.67**	**1.7**
Min. Shape	1.13	1.07	1.1	1.06
Max. Shape	9.09	8.75	5.14	7.1

Looking at the volume occupied by pigment versus pores (binder and voids) (Fig. 10 and Table 6), sample **M1** has a pigment content of 46.8% and sample **R1** of 43.1%. In the samples prepared with commercial synthetic ultramarine blue, the pigment occupies 47.2% of the volume in sample **R2** and 61.2% in sample **R3**. Sample **R3** has the lowest porosity (binder and voids), due to compact pigment packing, as a result of the presence of many very small particles (Fig. 9, Table 5).

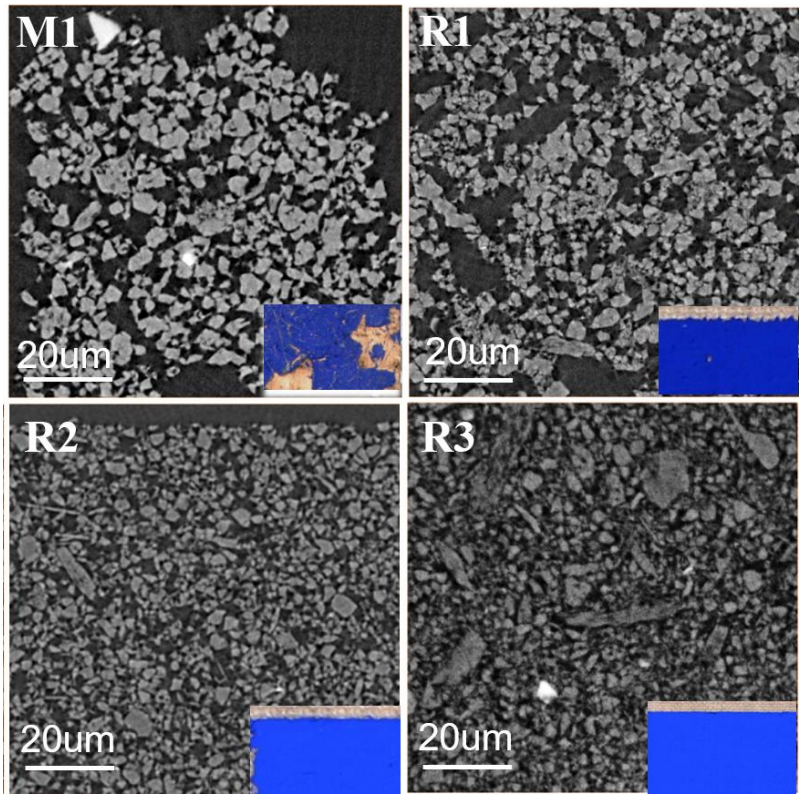

Fig. 10. Unrendered sectional images of reconstructed nano CT scans of paint sample M1, R1, R2 and R3 and small detail images (bottom right) of the paint layers the samples were retrieved from

Table 6. Statistics of NanoCT data analysis with volume quantities of M1, R1, R2 and R3

Pigment Type	Beach Landscape with Trees and Boats	Synt. ultramarine pigment MUNCH collection	Synt. ultramarine blue pigment dark	Synt. ultramarine blue pigment very dark
Binding Medium Type		Casein binder 3% in water 1:2 w/w pigment		
Sample No.	**M1**	**R1**	**R2**	**R3**
Volume Quantity Pores + Binder	53.2%	56.9%	52.8%	38.8%
Volume Quantity Pigment	46.8%	43.1%	47.2%	61.2%

None of the reconstructions shows the same particle size and porosity profile as the original sample. The model system that comes closest to the original **M1** is **R1**, prepared with a small amount of the loose synthetic ultramarine blue pigment, sampled from the MUNCH's historical material collection. From the mock-ups prepared with the commercial synthetic ultramarine blue pigments, **R2** (#45010 *Kremer Pigmente)*, is the one that has more comparable

properties to **M1**. **R3** (#45000, *Kremer Pigmente*) has the most distinct properties to those of **M1**.

Since a large number of mock-ups had to be prepared for the planned experiments it would have not been possible or ethical to use the loose pigment from the MUNCH's historical material collection. Therefore, the second-best matching mock-up system prepared with synthetic ultramarine dark (**R2**, #45000, *Kremer Pigmente*) was selected to produce 65 mock-ups (Fig. 11).

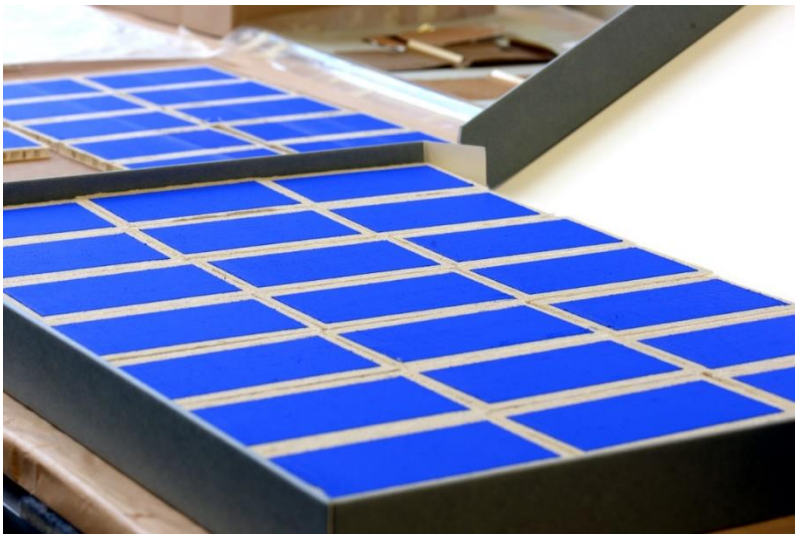

Fig. 11. Final paint-mock-ups prepared with synt. ultramarine pigment dark (#45010) and casein 3% 2:1 (w/w) on flax canvas used for the testing of consolidation materials and methods [13]

Conclusions

Material characterisation including fibre analysis and canvas weave structure analysis, pigments and binder identification, pigment-binder ratio calculation and total porosity determination of microsamples collected from the dark blue area in the painting entitled "Beach Landscape with Trees and Boats" (Woll M 637), 1905-06, by Edvard Munch were used for the preparation and selection of the most suitable model system for the development and optimization of a potential consolidation treatment of the target layer.

The results allowed for the preparation of 65 mock-ups with cohesively weak and porous paint layers with a similar total porosity and chemistry to the paint layer upon which it was based. Final paint-mock-ups were prepared with synthetic ultramarine blue pigment dark (#45010, *Kremer Pigmente)* and casein (#7555.2, *Carl Roth*) 3% 2:1 (w/w) in water on flax canvas.

Measurements of the pigment-binder ratio showed that the binder distribution within paint layers prepared with self-made paints is not homogenous. It should therefore be highlighted that due to the limited availability of sample material the results obtained on morphology and pigment-binder ration might not be statistically representative for the entire paint layer.

The modern commercially available synthetic ultramarine blue pigments examined have distinct particle size distribution to that found in the sample originating from MUNCH's historical material collection and the micro sample collected from the painting. Although comparable total porosity could be obtained, the tortuosity and effective porosity is most likely quite distinct due to the differing average particle size and particle size distribution.

The prepared mock-ups are nevertheless suitable model systems that allow for systematic comparison of different consolidation methods and materials. The results of the comparative research into the influence of the physico-chemical properties of the consolidant solutions and

the application method on the imbibition depth and time in the here developed model systems can be read in [13].

Authors contribution

This publication entails parts of the investigations performed in the context of Charlotte N. Stahmann's master's thesis, which was submitted in February 2021 at the Cologne Institute of Conservation Sciences at the Cologne University of Applied Sciences. The master's thesis was supervised by Prof. Dr. E. S. B. Ferreira and Dipl. Rest. Petra Demuth and both contributed to the development and design of the project. E. S. B. Ferreira further contributed to the drafting and writing of the manuscript. Dominik Müller performed nano CT measurements, data processing and analysis. Eva Storevik Tveit participated in the selection of the case study "Beach Landscape with Trees and Boats". All co-authors read and made editorial comments to the paper.

Acknowledgments

The authors would like to acknowledge Jennifer Poulin (Canadian Conservation Institute (CCI), Ottawa, Canada) for the Py-GC-MS analysis of the binder.

References

[1] L. Porsmo Stoveland, *Soiling removal from painted mock-ups, evaluation of novel surface cleaning methods on oil paint and chalk-glue ground in the context of the unvarnished Aula paintings by Edvard Munch*, **PhD Thesis**, University of Oslo, 2021.

[2] L. Porsmo Stoveland, B. Ormsby, M. Stols-Witlox, T. Frøysaker, F. Caruso, *Designing Paint Mock-Ups for a Study of Novel Surface Cleaning Techniques for Munch's Unvarnished Aula paintings*, **Conservation of Modern Oil Paintings** (Editors: K.J. van den Berg, I. Bonaduce, A. Burnstock, B. Ormsby, M. Scharff, L. Carlyle, G. Heydenreich, K. Keune), Springer International Publishing, 2019, pp. 553-563.

[3] L. Porsmo Stoveland, M. Stols-Witlox, B. Ormsby, N.L.W. Streeton, *Mock-ups and materiality in conservation research*, **Transcending Boundaries: Integrated Approaches to Conservation, ICOM-CC 19th Triennial Conference Beijing Preprints, Beijing 17-21 May 2021** (Editor: J. Bridgeland), International Council of Museums, Paris, 2021, pp. 1-14.

[4] E.S.B. Ferreira, K. Wyss, V. de Villemereuil, K. Beltinger, F. Marone, N.C. Scherrer, S. Zumbühl, *The role of the reconstructions in the identification of a wax/resin/gum tempera binder developed by Hermann Urban in 1901 and used by Cuno Amiet in 1902*, **Painting with Tempera, c. 1900 (**Editors: Karoline Beltinger, Jilleen Nadolny), Archetype Publications and SIK-ISEA, 2016, pp. 206-227.

[5] L. Carlyle, *Reconstructions of Oil Painting Materials and Techniques: The HART Model for Approaching Historical Accuracy*, **Reconstruction, Replication and Re-enactment in the Humanities and Social Sciences** (Editors: S. Dupré, A. Harris, J. Kursell, P. Lulof, M. Stols-Witlox), Amsterdam: Amsterdam University Press, 2021, pp. 169-198.

[6] M. Stols-Witlox, *Imperfect copies. Reconstructions in conservation research and practice*, **Reconstruction, Replication and Re-enactment in the Humanities and Social Sciences** (Editors: S. Dupré, A. Harris, J. Kursell, P. Lulof, M. Stols-Witlox), Amsterdam: Amsterdam University Press, 2021, pp. 169-198.

[7] L. Carlyle, *Historically Accurate Reconstructions of Oil Painters' Materials: An overview of the Hart Project 2002-2005*, **Reporting Highlights of the De Mayerne Programme, Research programme on molecular studies in conservation and technical studies in art**

history (Editors: J.J.Boon, E.S.B. Ferreira), NWO, The Hague, November 2006, pp. 63.-76.

[8] M. Beerse, K. Keune, P. Iedema, S. Woutersen, J. Hermans, *Evolution of Zinc Carboxylate Species in Oil Paint Ionomers*, **ACS Applied Polymer Materials, 2**(12), 2020, pp. 5674-5685. DOI: 10.1021/acsapm.0c00979.

[9] L. Baij, L. Chassouant, J.J. Hermans, K. Keune, P.D. Iedema, *The concentration and origins of carboxylic acid groups in oil paint*, **RSC Advances, 9**(61), 2019, pp. 35559-35564. DOI: 10.1039/c9ra06776k.

[10] J.J. Hermans, K. Keune, A. van Loon, P.D. Iedema, *An infrared spectroscopic study of the nature of zinc carboxylates in oil paintings*, **Journal of Analytical Atomic Spectrometry**, **30**(7), 2015, pp. 1600-1608. DOI: 10.1039/c5ja00120j.

[11] H. Wilks, **Adhesives and Coatings. Science for Conservators** *Book 3*, Conservation Science Teaching Series, London, 1987.

[12] S. Michalski, *physics model of the consolidation process, particularly of paintings,* **Proceedings of CESMAR7 Conference: The Care of Painted Surfaces. Materials and Methods for Consolidation and Scientific Methods to Evaluate their Effectiveness Milan November 2006, Colour and Conservation**, 2008, pp. 27-47

[13] C.N. Stahmann, K. Soppa, B. Glüsen, E.S. Tveit, A.T.F. Käckel, P. Demuth, E.S.B Ferreira, *Low-molecular-weight cellulose ethers as aerosols for the consolidation of cohesively weak paint layers*, **International Journal of Conservation Science, 13,** Special Issue 1, 2022, pp. 1583-1602.

[14] G. Woll, **Catalogue Raisonné Edvard Munch**, London 2009, pp. 653, 721.

[15] E.G. Sandbakken, E.S. Tveit, *Preserving a Master: Edvard Munch & His Painted Sketches*, **Journal of Urban Culture Research, 5**, 2012, DOI: https://doi.org/10.14456/jucr.2012.7.

[16] E.G. Sandbakken, E.S. Tveit, *Edvard Munch's monumental sketches (1909–1916) for the Aula of Oslo University, Norway: Conservation issues and treatments,* **Studies in Conservation, 57**, 2012, pp. 258-267.

[17] E. Hansen, M. H. Bishop, *Factors Affecting the Re-Treatment of Previously Consolidated Matte Painted Wooden Objects*, **Painted Wood: History and Conservation, Scientific Research Part 6,** Los Angeles, The Getty Conservation Institute, 1998, pp.484-497.

[18] P. Dietemann, U. Baumer, *Im Fokus - Bindemittel und Farbwirkung bei Kirchner*,**"Keiner hat diese Farben wie ich.' Kirchner malt**, Kirchner Museum Davos, Hatje Cantz Verlag, Ostfilder, 2011, pp. 40-41.

[19] A. Callen, **The Art of Impressionism: Painting Technique & the Making of Modernity**, Yale University Press, 2000.

[20] V. Jirat-Wasiutynski, H. Travers Newton, *Absorbent grounds and the matt aesthetic in Post-Impressionist painting*, **Studies in Conservation**, 1998, pp. 235-239.

[21] E. Hummert, U. Henniges, A. Potthast, *Stabilisation Treatments with Aerosols. Evaluating the Penetration Behaviour of Gelatine and Methylcellulose*, **Restaurator International Journal for the Preservation of Library and Archival Material, 34**(2), 2013, pp. 134-171. DOI: 10.1515/res-2013-0008.

[22] S. Patari, P. S. Mahapatra, *Imbibition of Liquids through a Paper Substrate in a Controlled Environment*, **Langmuir 38**(15), 2022, pp. 4736-4746.

[23] K. Weishaupt, *Model Concepts for Coupling Free Flow with Porous Medium Flow at the Pore-Network Scale: From Single-Phase Flow to Compositional Non-Isothermal Two-Phase Flow*, **PhD Thesis**, Institut für Wasser- und Umweltsystemmodellierung der Universität Stuttgart, 2020.

[24] J. Perko, R. Zarzuela, I. Garcia-Lodeiro, M. T. Blanco-Varela, M. J. Mosquera, T. Seemann, L. Yu, *The importance of physical parameters for the penetration depth of impregnation products into cementitious materials: Modelling and experimental study*, **Construction and Building Materials, 257**, 2020, 119595.

[25] L. Bertrand, S. Bernard, F. Marone, M. Thoury, I. Reiche, A. Gourrier, P. Sciau, U. Bergmann, *Emerging Approaches in Synchrotron Studies of Materials from Cultural and Natural History Collections*, **Topic in Current Chemistry, 374**(1), 2016, Article Number: 7. DOI: 10.1007/s41061-015-0003-1.

[26] M. Cotte, A. Genty-Vincent, K. Janssens, J. Susini, *Applications of synchrotron x-ray nano-probes in the field of cultural heritage*, **Comptes Rendus Physique**, **19**(7), 2018, pp. 575-588. https://doi.org/10.1016/j.crhy.2018.07.002.

[27] C. Gervais, J.J. Boon, F. Marone, E.S.B. Ferreira, *Characterization of porosity in a 19th century painting ground by synchrotron radiation X-ray tomography*, **Applied Physics A., 111**(1), 2013, pp. 31-38.

[28] E.S.B. Ferreira, J.J. Boon, F. Marine, M. Stampanoni, *Study of the mechanisms of formation of calcium soaps in an early 20th century easel painting with correlative 2D and 3D microscopy*, **Proceedings of 16th Triennal Meeting ICOM Committee for Conservation, Lisbon September 2011**, James&James Publisher, 2011.

[29] J.J. Boon, E. Oberthaler, E.S.B. Ferreira, F. Marone, M. Stampanoni, *X-ray Tomographic Microscopic Studies a Resin Embedded Paint Sample from a Mechanical Failing Area in the Floor Tiles of The Art of Painting by Johannes Vermeer (1632-1675)*, **Microscopy and Microanalysis, 6**(16), 2012, pp. 1872-1873.

[30] E.S.B. Ferreira, J.J. Boon, J. van der Horst, N.C. Scherrer, F. Marone, M. Stampanoni, *3D Synchrotron x-ray microtomography of paint samples*, **O3A: Optics for Arts, Architecture, and Archaeology II** (Editor: L. Pezzati, R. Salimbeni), 2009.

[31] C. Jacobsen, **X-ray Microscopy**, Cambridge University Press, pp. 246-252

[32] F. Lutter, P. Stahlhut, K. Dremel, S. Zabler, J. Fell, H. Herrmann, R. Hanke, *Combining X-ray Nano Tomography with focused ion beam serial section imaging - Application of correlative tomography to integrated circuits*, **Nuclear Instruments and Methods in Physics Research Section B: Beam Interactions with Materials and Atoms**, **500**, 2021, pp. 10-17.

[33] D. Müller, J. Graetz, A. Balles, S. Stier, R. Hanke, C. Fella, *Laboratory-Based Nano-Computed Tomography and Examples of Its Application in the Field of Material Research*, **Crystals, 11**(6), 2021**,** Article Number: 677, DOI10.3390/cryst11060677.

[34] B.J. Rouba, *Die Leinwandstructuranalyse und ihre anwendung für die Gemäldekonservierung*, **Restauratorenblätter 13, Malerei und Textil**, 1993, pp. 79-89.

[35] E. Haugan, B. Holst, *Determining the fibrillar orientation of bast fibres with polarized light microscopy: the modified Herzog test (red plate test) explained*, **Journal of Microscopy, 252:2**, 2013, pp. 159-168.

[36] S. Wülfert, **Der Blick ins Bild**, First Edition, Urania, Freiburg, 1999, pp. 290, 352.

[37] M. R. Derrick, D. Stulik, J. M. Landry, **Infrared Spectroscopy in Conservation Science, Scientific Tools for Conservation**, The Getty Conservation Institute, Los Angeles 1999, p. 85.

[38] F. Casadio, L. Bellot-Gurlet, C. Paris, *Factors Affecting the Reactivity of Zinc Oxide with Different Drying Oils: A Vibrational Spectroscopy Study*, **Metal Soaps in Conservation**, 2019.

[39] R. Wiesinger, L. Pagnin, M. Anghelone, L. M. Moretto, E. F. Orsega, M. Schreiner, *Pigment and Binder Concentrations in Modern Paint Samples Determined by IR and Raman Spectroscopy*, **Angewande Chemie - International Edition, 57**(25), 2018, pp. 7401-7407, Special Issue SI, DOI: 10.1002/anie.201713413.

[40] J. Poulin; M. Kearney; M.A. Veall, *Direct Inlet Py-GC-MS Analysis of Cultural Heritage Materials*. **Journal of Analytical and Applied Pyrolysis, 164,** 2022, pp. 105506. https://doi.org/10.1016/j.jaap.2022.105506.

[41] H. Wang, S. Zhang, S. Hu, Z. Zhen, M. A. Gomez, S. Yao, *A systematic study of the synthesis conditions of blue and green ultramarine pigments via the reclamation of the industrial*

zeolite wastes and agricultural rice husks, **Environmental Science and Pollution Research, 27**, 2020, pp. 10910-10924.
[42] M. Doerner, **Malmaterial und seine Verwendung im Bilde**, Fully revised and expanded 19th edition, Stuttgart, 2001, p. 99.
[43] M. Ullherr, S. Zabler, J. Grätz, R. Hanke, *pyXIT: Python GUI Software for CT Imaging, Learning and Experimental Algorithms; Example: Multi Material Phase Retrieval*, **International Symposium on Digital Industrial Radiology and Computed Tomography**, 2-4 July 2019, Fürth, Germany.
[44] J.A. Suomela, K. Vajanto, R. Räisänen, *Seeking Nettle Textiles – Utilizing a Combination of Microscopic Methods for Fibre Identification*, **Studies in Conservation, 63**(7), 2018, pp. 412-422.
[45] S. Orsini, F. Parlanti, I. Bonaduce, *Analytical Pyrolysis of Proteins in Samples from Artistic and Archaeological Objects*, **Journal of Analytical and Applied Pyrolysis, 124**, 2017, pp. 643–657. https://doi.org/10.1016/j.jaap.2016.12.017.
[46] J.-H. Wang, C.-S. Quan, X.-H. Qi, X. Li, S.-D. Fan, *Determination of Diketopiperazines of Burkholderia Cepacia CF-66 by Gas Chromatography–Mass* Spectrometry, **Analytical and Bioanalytical Chemistry, 396**(5), 2010, pp. 1773–1779. https://doi.org/10.1007/s00216-009-3379-3.
[47] J. Poulin, D. Duguay, *Analyse Supplémentaire de Traces de Peinture Sur Un Buffet*, **Unpublished Report**, Canadian Conservation Institute, 2014.
[48] I.C.A Sandu, E. G. Sandbakken, J. Ferrer, T. Syversen, A. Hull, *The art historical materials collection at MUNCH: colors, brands, labels*, **International Journal of Conservation Science, 13,** Special Issue 1, 2022, pp. 1653-1664.
[49] E.G. Sandbakken, E. Chan, H. Kutzke, L. Puskar, I.C.A Sandu, *Powdery Pigments from original materials collection of Munch: conservation treatment and analytical characterization*, **International Journal of Conservation Science, 13,** Special Issue 1, 2022, pp. 1681-1690.
[50] C. Gierløff, **Edvard Munch Selv**, Gyldendal Oslo, 1953, pp. 205, 208.

Received: May 12, 2022
Accepted: December 24, 2022